Modeling Permeation of Binary Mixtures Through Zeolite Membranes

Jolinde M. van de Graaf, Freek Kapteijn, and Jacob A. Moulijn
Delft University of Technology, Faculty of Applied Sciences, Waterman Institute for Precision Chemical Engineering, Section Industrial Catalysis, Julianalaan 136, 2628 BL Delft, The Netherlands

The separation of ethane/methane and propane/methane mixtures with a silicalite-1 membrane was investigated as a function of composition, total hydrocarbon pressure (up to 425 kPa), and temperature (273–373 K). The selectivity of the membrane is highly dependent on these operating conditions. The generalized Maxwell–Stefan equations were used to predict the fluxes and the associated selectivities. These model predictions, based on separately determined single-component adsorption and diffusion parameters, were in excellent agreement with the experimental data. Using the empirical Vignes relation for the prediction of the binary Maxwell–Stefan surface diffusivity, there were no fitting parameters involved in the model prediction. The importance of incorporation of adsorbate–adsorbate interactions in the model is clearly shown, both for transient and steady-state mixture permeation. Theoretical analysis showed that for mixtures of a fast, weakly adsorbing component and a slow, strongly adsorbing component the maximum selectivity obtained with microporous membrane separation is always a factor of 2 lower than the one obtained under equilibrium adsorption conditions.

Introduction

The application of molecular sieve materials, such as carbon molecular sieves and zeolites, in gas-separation and -purification processes offers interesting alternatives for conventional separation technology. The pores of these materials are near molecular dimensions, enabling separation of components on the basis of differences in adsorption or differences in shape. Molecular sieves can be used as adsorbents in pressure-swing adsorption (PSA) or temperature-swing adsorption processes, or they can be used in the form of membranes. Both process configurations have high potential for specific applications depending on the desired product, the desired product purity, the feasibility of operation and economics. For example, the kinetic separation of air with PSA is practiced on a large scale using carbon molecular sieves (Knoblauch, 1978; Knoblauch et al., 1985). Karpoor and Yang (1989) suggested a kinetic PSA process for methane/CO_2 separation, using a carbon molecular sieve as adsorbent. Rao and Sircar (1993) studied the feasibility of a hybrid PSA/membrane system for the recovery of hydrogen from refinery waste gases, making use of the adsorption selectivity of a carbon molecular sieve membrane.

Zeolite membranes have shown interesting separation characteristics, such as the separation of hydrocarbon isomers (Funke et al., 1996; Kusakabe et al., 1996; Vroon et al., 1998) or the separation of strongly from weakly adsorbing components (Geus et al., 1993; Jia et al., 1994; Kapteijn et al., 1995; Vroon et al., 1996; Bakker et al., 1996; Kusakabe et al., 1997; Poshusta et al., 1998; Kusakabe et al., 1998; Van de Graaf et al., 1998a). The separation performance of zeolite membranes is highly dependent on operating conditions such as temperature, total pressure, and composition (Van de Graaf et al., 1998a). In a membrane separation unit temperature and pressure are usually constant and knowledge about the separation features of the zeolite membrane is required to choose the optimal conditions. The composition of a mixture changes throughout the separation unit until the desired purity is achieved. For the proper design of separation units the composition dependence of the selectivity is thus an important factor.

Prediction of the separation performance of molecular sieve membranes requires knowledge on multicomponent adsorption and diffusion models in microporous materials. Ide-

Correspondence concerning this article should be addressed to J. M. van de Graaf.
Current address of J. M. van de Graaf: Shell Global Solutions, Shell Treating Services, P.O. Box 38000 1030 BN, Amsterdam, The Netherlands.

ally, one would like to predict mixture permeation under a variety of conditions, based on single-component parameters. Despite the practical importance of the theoretical description of multicomponent mass transfer in microporous membranes, the number of studies that address this issue is limited. One of the main questions that arises when modeling multicomponent surface diffusion in zeolites is whether or not adsorbate–adsorbate interactions have to be included and how.

Krishna applied the generalized Maxwell–Stefan equations to multicomponent surface diffusion (Krishna, 1990, 1993). In this model cross-term diffusivities, accounting for molecule–molecule interactions, are estimated using an empirical relationship given by Vignes (1966).

Chen and Yang (1992) used a kinetic approach to calculate the Fickian diffusivity matrix for surface diffusion of multicomponent systems. In this approach a blocking parameter λ_{ii} that represents the extent of blocking of the pore by coadsorbed molecules was introduced. The value of λ_{ii} is related to the interaction energies between molecules and between molecules and a vacant site. For $\lambda_{ii} = 0$, this kinetic model yields the same equation as the Maxwell–Stefan equations with vanishing cross-terms.

The theory of irreversible thermodynamics with vanishing cross-coefficients was used by Habgood (1958) and Kärger and Bülow (1975) for describing binary uptake measurements in zeolite crystals. Habgood (1958) showed that this theory predicted the observed maximum in the adsorbed phase concentration of the weakly adsorbing component as a function of time qualitatively. In the work of Kärger and Bülow (1975) this theory failed to describe the initial stages of adsorption, but it had good predictive power after the initial step. Yang et al. (1991) derived an expression for the cross-term coefficients in the theory of irreversible thermodynamics and included these cross-coefficients in the prediction of binary diffusion in zeolites. These cross-term coefficients significantly influence the calculated uptake rates of CO_2 and methane in zeolite-4A. However, from comparison with the available experimental data, no clear conclusion could be drawn if these effects should be included in the model prediction.

The kinetic model of Chen and Yang (1992) was used to describe mixture permeation of methane and ethane through a carbon molecular sieve membrane based on single-component diffusivities (Chen and Yang, 1994). The blocking parameters in the mixture were also predicted from single-component permeation experiments. Although the binary model underestimated the ethane flux in the mixtures, the results indicated that the cross-term diffusivities could not be neglected.

The Maxwell–Stefan approach without cross-term diffusivities was used to describe the contribution of surface diffusion to the permeation of propane/CO_2 mixtures through a mesoporous glass membrane with a pore diameter of ~ 4 nm (Tuchlenski et al., 1998). In this type of membrane gas-phase diffusion and surface diffusion occur parallel, and surface diffusion amounted to $\sim 40\%$ of the total flux at 293 K. The accuracy of the prediction of mixture diffusion was found to depend heavily on the description of the multicomponent adsorption equilibrium.

Mixture permeation through zeolite membranes has only been modeled qualitatively (Krishna and Van den Broeke, 1995; Kapteijn et al., 1995) using the generalized Maxwell–Stefan equations without adsorbate–adsorbate interactions. In these studies it was shown that the generalized Maxwell–Stefan equations provide a sound basis for the description of multicomponent mass transfer through this type of membrane, while the Fick formulation fails to describe the qualitative features of zeolite membrane permeation. Up to now, no attempts have been made to describe the separation performance of zeolite membranes quantitatively.

The generalized Maxwell–Stefan equations were chosen as the starting point for modeling of multicomponent permeation through the silicalite-1 membrane used in this study. Hitherto, the adsorbate–adsorbate interaction terms in the Maxwell–Stefan equations have always been neglected for the description of mixture permeation through microporous membranes (Krishna and Van den Broeke, 1995; Kapteijn et al., 1995). The assumption that these interactions are negligible, however, has never been verified experimentally. The aim of this study is to predict the separation performance of a silicalite-1 membrane under a variety of operating conditions, such as temperature and pressure, based on single-component diffusion data. The contribution of adsorbate–adsorbate interactions will be evaluated by comparing model predictions with and without interaction terms with experimental data.

Experimental

Membrane synthesis

The composite membrane used in this study consisted of a thin top layer of silicalite-1 with an effective thickness of 10 μm, supported on a stainless-steel support (SIKA-RF, Krebsöge). The support itself was a composite composed of metal wool (thickness: 200 μm; porosity ~ 0.7) and sintered stainless-steel spheres (thickness: 3 mm; porosity: 0.2). Synthesis of the zeolite layer on top of the support was done by crystallization under autogenous pressure. A flat-sheet silicalite-1 membrane was obtained (surface area: 2.0×10^{-4} m^2) exhibiting a good permselectivity for *n*-butane to *i*-butane permeation (~ 25). For further details on the synthesis procedures see Geus et al. (1993) and Van de Graaf et al. (1998b).

Permeation experiments

Permeation experiments with methane (99.95%), ethane (99.95%), propane (99.95%), and ethane/methane and propane/methane mixtures were performed according to the Wicke–Kallenbach principle, employing a sweep gas (helium, 99.999%, 100×10^{-6} m$^3 \cdot$ min^{-1} STP) at the permeate side to remove the permeating components. Both the feed and the sweep stream were delivered to the membrane cell through spray heads, ensuring that the volumes at each side of the membrane were well mixed. Single-component permeation experiments were performed using the pure hydrocarbon or, to obtain partial pressures lower than atmospheric, mixtures of the hydrocarbon balanced with helium to 101 kPa.

Mixture permeation experiments were performed (1) as a function of *composition*, keeping the total hydrocarbon pressure at the feed side atmospheric, (2) as a function of *pressure*, keeping the ratio between components the same and

increasing the total pressure at the feed side, and (3) as a function of *temperature*.

The total feed flow was between 70×10^{-6} $m^3\cdot min^{-1}$ (STP) and 100×10^{-6} $m^3\cdot min^{-1}$ (STP).

The composition of the permeate was analyzed with a mass spectrometer (Ledamass quadrupole analyzer). Before each set of experiments the membrane was outgassed at 623 K overnight under flowing helium at both sides.

Theory

Figure 1 shows the module used in permeation experiments. Four regions can be distinguished: the retentate volume, the zeolite layer, the support layer, and the permeate volume. For the accurate modeling of mixture permeation through the composite membrane the concentrations and/or concentration profiles of all components in each region have to be calculated.

The retentate and permeate volumes are considered to be well mixed, which implies that the concentration in these volumes is identical to the concentrations in the outlet flows. The retentate composition can deviate considerably from the feed composition since the retentate is enriched in the retained component and depleted in the fastest permeating component.

In general, back permeation and the presence of the sweep gas can lower the flux through the zeolite layer (Van de Graaf et al., 1998b). However, models that account for interaction between molecules that do not adsorb in the zeolite in measurable quantities, such as helium, and adsorbed molecules still have to be developed. At the relatively low temperatures of these experiments (273–373 K) the counterflux of the sweep gas is very low, and therefore neglected in the calculations. If there is an effect of the sweep gas in this study, this effect is lumped in the value of the diffusivity calculated from single-component experiments.

The retentate composition of a binary mixture can be calculated from a mass balance over the feed volume, which according to Eq. 1, is considered to be a well-mixed volume

$$\frac{p_{i,\mathrm{ret}}}{p_{\mathrm{ret}}^{\mathrm{tot}}}=\frac{\phi_{i,\mathrm{feed}}-N_i\cdot A}{\phi_{\mathrm{feed}}^{\mathrm{tot}}-\sum_{i=1..n}N_i\cdot A}. \tag{1}$$

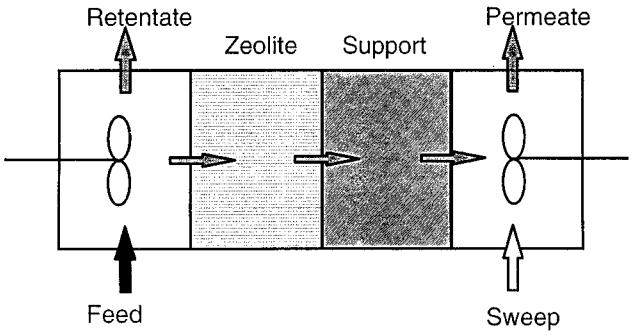

Figure 1. The permeation module.

The permeate partial pressure in the permeate volume can be calculated in a similar way.

The selectivity of the membrane is defined in Eq. 2 as the ratio between the quotient of the permeate mol fractions and the quotient of the retentate mole fractions:

$$\alpha_{ij}=\frac{y_{i,\mathrm{perm}}/y_{j,\mathrm{perm}}}{y_{i,\mathrm{ret}}/y_{\mathrm{j,ret}}}. \tag{2}$$

It should be noted that this selectivity is different from the one determined by the ratio between the permeances that is also used in membrane separation.

Transport in the zeolite layer

In a layer of randomly intergrown zeolite crystals it is almost inavoidable that some intercrystalline, nonzeolitic pores exist. For the membrane used in this study a small flux of tri-isopropyl benzene (4.6×10^{-8} $mol\cdot m^{-2}\cdot s^{-1}$ at the vapor pressure) has been observed (Van de Graaf, 1998c). This points to the existence of a small number of pores that are larger than the zeolitic pores, since tri-isopropyl benzene has a kinetic diameter of 0.85 nm compared to a pore aperture of $\sim$0.55 nm for silicalite-1. The size of these nonzeolitic pores has been estimated to be 2 to 3 times the zeolitic pores (Van de Graaf, 1998c). This estimation is based on the absence of a viscous flow contribution to the permeance of helium and neon at temperatures above 273 K and the limited counter-diffusion of the helium sweep gas in the presence of an adsorbing component. The contribution of these nonzeolitic pores to overall permeation is strongly dependent on the transport mechanism prevailing in these pores for the component under study. Under the conditions used in this study ($T<373$ K), diffusion of the adsorbing components through intercrystalline regions in the membrane will mainly occur by surface diffusion. Although surface diffusion in these larger pores is expected to be different from surface diffusion in the zeolitic pores, the qualitative behavior will be the same. This makes it impossible to take permeation through nonzeolitic pores into account separately. These contributions are therefore lumped in the modeling.

The generalized Maxwell–Stefan equations provide an adequate basis for the description of multicomponent mass transfer in porous media (Krishna, 1993). The Maxwell–Stefan formulation is equivalent to the Onsager formulation derived from irreversible thermodynamics. The Maxwell–Stefan formulation is a convenient way to describe diffusion in porous media and yields coefficients that are directly amenable to physical interpretation. The pros and cons of the different approaches are discussed by Wesseling and Krishna (1991). The basis of the Maxwell–Stefan theory is that the driving force for movement that is acting on a species is balanced by the friction that is experienced by that species. This approach was applied to surface diffusion in microporous media by Krishna (Krishna, 1990).

Transport of hydrocarbons in the zeolite layer is proceeding by surface diffusion under the conditions used in this study ($T<373$ K) (Bakker et al., 1997). The general form of the generalized Maxwell–Stefan equations applied to surface dif-

fusion is given by Eq. 3

$$-\frac{\theta_i}{RT}\nabla\mu_i = \sum_{j=1}^{n}\frac{\theta_j N_i^s - \theta_i N_j^s}{q_{\text{sat}}\cdot\rho\cdot\mathcal{D}_{ij}^s} + \frac{N_i^s}{q_{\text{sat}}\cdot\rho\cdot\mathcal{D}_i^s}, \qquad i,j=1,2,\ldots,n. \quad (3)$$

The driving force for diffusion is the chemical potential gradient ($\nabla\mu_i$) on the lefthand side of Eq. 3. Friction is the result from interactions between adsorbed molecules (first term on the righthand side) and interaction between a molecule and the pore wall (second term on the righthand side). The parameters $\mathcal{D}_{ij}^s$ and $\mathcal{D}_i^s$ are the Maxwell–Stefan surface diffusivities and represent inverse friction factors between molecules and between molecules and the wall, respectively. If there is no friction with the wall or with other molecules, the respective Maxwell–Stefan surface diffusivities are large and the corresponding term in Eq. 3 vanishes.

The chemical potential gradient can be related to the gradient in the surface coverage by a matrix of thermodynamic factors (Krishna, 1990)

$$\frac{\theta_i}{RT}\nabla\mu_i = \sum_{j=1}^{n}\Gamma_{ij}\nabla\theta_i \quad \text{where} \quad \Gamma_{ij} \equiv \theta_i\frac{\partial \ln p_i}{\partial\theta_j}, \qquad i,j=1,2,\ldots,n. \quad (4)$$

The surface occupancy, θ_i, is related to the partial pressure by the adsorption isotherm. The choice of the adsorption model determines the mathematical form of the thermodynamic factor. In this study the extended Langmuir equation was used (Eq. 5)

$$\theta_i = \frac{q_i}{q_{sat}} = \frac{K_i p_i}{1+\sum_{j=1}^{n} K_j p_j} \qquad i,j=1,2,\ldots,n. \quad (5)$$

The extended Langmuir equation was used for its mathematical simplicity in this study, but other models, such as the Ideal Adsorbed Solution Theory developed by Meyers and Prausnitz (1965), may be more adequate, especially for more complex systems than the ones studied here.

The combination of Eqs. 3–5 gives the surface flux of a component through the membrane in a multicomponent system. Equation 6 and Eq. 7 represent the expressions for a unary and a binary system, respectively

$$N_i^s = -q_{\text{sat}}\,\rho\cdot\frac{\mathcal{D}_i^s}{1-\theta_i}\cdot\nabla\theta_i \quad (6)$$

$$N_1^s = -q_{\text{sat}}\,\rho\frac{\mathcal{D}_1^s}{(1-\theta_1-\theta_2)} \times \frac{\left[(1-\theta_2)+\theta_1\frac{\mathcal{D}_2^s}{\mathcal{D}_{12}^s}\right]\nabla\theta_1 + \left[\theta_1+\theta_1\frac{\mathcal{D}_2^s}{\mathcal{D}_{12}^s}\right]\nabla\theta_2}{\theta_2\frac{\mathcal{D}_1^s}{\mathcal{D}_{12}^s}+\theta_1\frac{\mathcal{D}_2^s}{\mathcal{D}_{12}^s}+1}. \quad (7)$$

A special case of Eq. 7 is when friction between molecules is much less important than friction with the wall. In that case $\mathcal{D}_{ij}^s$ is much larger than $\mathcal{D}_i^s$, and Eq. 7 reduces to

$$N_1^s = -q_{\text{sat}}\,\rho\frac{\mathcal{D}_1^s}{(1-\theta_1-\theta_2)}\left[(1-\theta_2)\nabla\theta_1+\theta_1\nabla\theta_2\right], \quad (8)$$

which is referred to as the "single-file" diffusion mode (Krishna, 1993).

Equation 6, for single-component diffusion, is the same as the often used Darken equation (Kärger and Ruthven, 1992). The Darken equation is used to correct the Fickian diffusivity, based on the concentration gradient as the driving force for diffusion, for the true driving force for diffusion, the chemical potential gradient. This yields the so-called corrected diffusivity, whereas the Fick diffusivity is referred to as an apparent diffusivity. The corrected diffusivity from the Darken equation is identical to the Maxwell–Stefan diffusivity. The corrected diffusivity is often assumed to be independent of occupancy, but this does not necessarily have to be the case (Van den Broeke, 1995; Krylov et al., 1997). The Maxwell–Stefan surface diffusivity $\mathcal{D}_i^s$ and its concentration dependence can be calculated from single-component permeation experiments, if the adsorption parameters are known.

Equation 8 corresponds to the Onsager formalism of irreversible thermodynamics with vanishing cross-term coefficients, in combination with Langmuir adsorption (Van den Broeke, 1995). This formulation, without adsorbate–adsorbate interactions, has frequently been used to describe the uptake of binary mixtures in zeolites (Habgood, 1958; Kärger and Bülow, 1975). If the single-component Maxwell–Stefan diffusivities are independent of occupancy and the friction between molecules can be neglected, Eq. 8 can be used to predict the permeation of a binary mixture based solely on single-component diffusion and adsorption parameters, provided that the extended Langmuir equation is valid.

If molecule–molecule interactions cannot be neglected, Eq. 7 can be used. Determining the cross-term diffusivities $\mathcal{D}_{ij}^s$ is subject to discussion (Yang et al., 1991). Krishna (1990) proposed to use the empirical relation of Vignes (1966) to determine $\mathcal{D}_{ij}^s$ from the single-component diffusivities (Eq. 9):

$$\mathcal{D}_{ij}^s = \mathcal{D}_i^{s\,\theta_i/(\theta_i+\theta_j)}\mathcal{D}_j^{s\,\theta_j/(\theta_i+\theta_j)}. \quad (9)$$

The cross-term diffusivities satisfy the Onsager reciprocity relation (Krishna, 1990)

$$\mathcal{D}_{ij}^s = \mathcal{D}_{ji}^s. \quad (10)$$

In this study the predictive power of the Maxwell–Stefan equations without adsorbate–adsorbate interactions [further referred to as GMS($\mathcal{D}_{ij}^s=\infty$), Eq. 8] and the ones including adsorbate–adsorbate interactions (further referred to as GMS, Eqs. 7 and 9) will be analyzed based on single-component adsorption and diffusion parameters. Single-component diffusion parameters are derived from single-component permeation experiments, using Eq. 7 and correcting for the support

influence. Single-component adsorption data are available in literature (Zhu et al., 1998). The predictions for binary mixture permeation using the GMS model and the GMS($Đ_{ij}^{s} = \infty$) model are verified with experimental data.

Support layer

The resistance of the support layer cannot be neglected. Although diffusion in the support is relatively fast compared to diffusion in the zeolite layer, the support causes a substantial partial-pressure gradient due to its thickness (3 mm) and its low porosity (0.2). This affects the boundary condition at the zeolite/support interface, and it is therefore important to take the partial-pressure gradient across the support into account (Van de Graaf et al., 1998b).

For the calculation of the partial-pressure gradient in the support layer the Maxwell–Stefan equations can be used, with a general form comparable to Eq. 3, now applied to gas-phase diffusion (Krishna, 1993), which is generally accepted to describe multicomponent mass transfer (see special issue of *Chem. Eng. J.*, 1995). In the Wicke–Kallenbach experiments molecular diffusion prevails in the support layer and molecule–wall interactions, and viscous flow can be neglected. The partial-pressure gradient across the support layer can then be described by Eq. 11

$$-\frac{1}{RT}\nabla p_i = \sum_{j=1}^{n} \frac{y_j N_i - y_i N_j}{\epsilon \cdot Đ_{ij}} \quad i, j = 1..n. \tag{11}$$

In the permeation experiments of binary mixtures, three components have to be included in the calculations: the two feed components and the sweep gas, helium. As mentioned earlier, the counterflux of helium was neglected. The value of the binary molecular diffusivity, $Đ_{ij}$, can be calculated from correlations in the literature, for example, the one of Füller et al. (1966). The values for the gas-phase diffusivities are listed in Table 1.

Adsorption parameters

The adsorption parameters for the components under study were obtained from the work of Zhu et al. (1998). These data were obtained with a silicalite-1 sample that was calcined in the same way as the membrane used in this study. Figure 2 shows the isotherms of methane, ethane, and propane at 303 K. It was found that (1) the single-component adsorption isotherms of methane, ethane, and propane follow a type I adsorption isotherm according to the Brunauer classification, and (2) the saturation capacity of the zeolite is temperature-dependent (Zhu et al., 1998).

For thermodynamic consistency of the extended Langmuir equation, the saturation capacity for each component in a binary pair must be the same (Broughton, 1948). As can be seen in Figure 2, this thermodynamic requirement for the extended Langmuir equation is not satisfied. In the derivation of Eqs. 7 and 8 it was also assumed that the saturation capacity is identical for both components. In order to be consistent, a constant adsorption capacity was assumed for competitive adsorption of ethane and methane and of propane and methane, although this led to a less accurate description of the methane adsorption equilibrium data (Figure 2). It was found that the assumption of constant saturation capacity had only a minor influence on the final calculation results.

Table 1. Diffusion Parameters

	Zeolite Layer*	Support Layer**		
	$Đ_i^s$	$Đ_{i,he}$	$Đ_{C_1,C_2}$	$Đ_{C_1,C_3}$
	[10^{-10} m^2·s^{-1}]	[10^{-5} m^2·s^{-1}]	[10^{-5} m^2·s^{-1}]	[10^{-5} m^2·s^{-1}]
Methane (C_1)				
273	8.64	5.6	1.4	
303	10.4	6.7	1.7	1.4
338	15.2	8.1	2.0	
373	20.7	9.6	2.4	
Ethane (C_2)				
273	0.95	4.0		
303	1.50	4.8		
338	3.14	5.8		
373	5.83	6.9		
Propane (C_3)				
303	0.34	3.9		

*Calculated from single-component permeation data, Eq. 6.
**Calculated from the empirical relation of Füller et al. (1996).

Abdul-Rehman et al. (1990) measured the adsorption of ethane, methane, propane, and mixtures thereof on silicalite-1. For ethane, methane, and ethane/methane mixture adsorption it was found that the (extended) Langmuir equation is adequate, even though the saturation capacities of the single components were different. For propane/methane mixtures some deviations were found upon predicting mixture adsorption with the extended Langmuir equation. The Toth isotherm was found to be more adequate in this case. The choice of the adsorption isotherm affects the concentration dependence of the diffusivity, as it influences the thermodynamic factor. However, in this case the Toth isotherm has only a minor effect on the concentration dependence of the

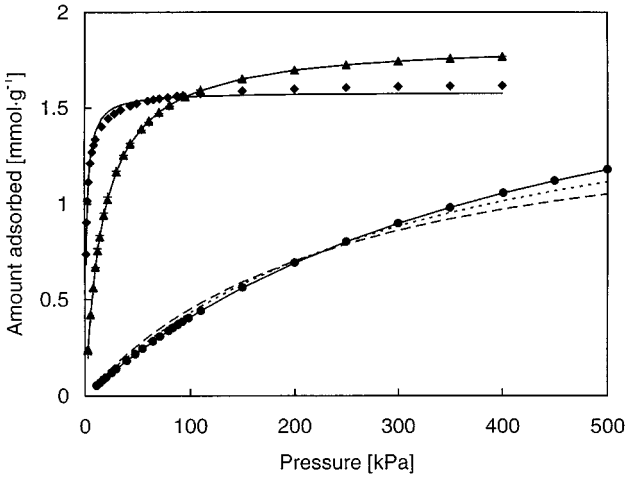

Figure 2. Adsorption isotherms of methane (●), ethane (▲), and propane (♦) at 303 K.

Solid lines represent the fits of the Langmuir equation (Eq. 5). For methane: dotted line $q_{sat,methane} = q_{sat,ethane}$; dashed line $q_{sat,methane} = q_{sat,propane}$. Symbols represent experimental data of Zhu et al. (1998).

single-component diffusivity, as the value of the Toth coefficient was found to be close to 1 (~ 0.83 for propane) (Abdul-Rehman et al., 1990). For values of the Toth coefficient close to one, the Toth isotherm is almost identical to the Langmuir isotherm. There are no kinks or steps in the (mixture) adsorption isotherms of the components in this study, which would be the case if surface heterogeneity would play a role (Zhu et al., 1998; Abdul-Rehman et al., 1990). For these simple systems, the extended Langmuir equation is therefore a good approximation. When the size of the molecules approaches that of the zeolite channels, for example, in the case of *i*-butane, there is a clear effect of the heterogeneity of the zeolite framework (Zhu et al., 1998; Smit and Maessen, 1995; Vlugt et al., 1998) and the Langmuir equation cannot be used.

The adsorption data were fitted with the Langmuir equation (Eq. 5) at 303 K, 338 K, and 373 K, the same temperatures as the permeation experiments. For ethane and propane the saturation capacity (q_{sat}) and the adsorption constant were estimated (K_i). For methane the value of K_i was estimated while using the fixed saturation capacity for ethane or propane. The values of q_{sat} and K_i for ethane and methane at 273 K were extrapolated from the data at higher temperatures assuming a linear relationship between the adsorption capacity and temperature and a van't Hoff-type relation for the adsorption constant.

Table 2 lists the adsorption parameters used to predict the surface occupancies in single-component and binary permeation experiments using the extended Langmuir equation.

Prediction of mixture permeation

Prediction of binary mixture permeation was done by calculating numerically the temporal development of the fluxes after a concentration-step exposure to the membrane, until steady-state values were obtained (Van de Graaf, 1998c). The relevant membrane parameters are listed in Table 3.

Results

Single-component permeation

Figure 3a gives the single-component fluxes of methane, ethane, and propane at 303 K as a function of the feed (partial) pressure. The flux of methane is linearly proportional to its feed (partial) pressure, but the fluxes of ethane and propane level off at higher pressures. At 373 K the flux of methane still shows a linear trend with feed (partial) pressure and that of ethane is much less curved than it is at 303 K (Figure 3b).

Due to the shape of the adsorption isotherm for strongly adsorbing components (Figure 2), increasing the feed pressure hardly results in an increase in the surface concentration at the feed side of the membrane at higher feed pressures. Consequently, the apparent driving force for diffusion, the surface concentration gradient (Eq. 6), does not increase linearly with the feed partial pressure. This is reflected in the nonlinear trend in the flux as a function of the feed partial pressure for ethane and propane at 303 K. At this temperature permeation is thus clearly dependent on the amount adsorbed, rather than on the feed pressure. This shows that diffusion of adsorbed species is involved. At higher temperature or for weakly adsorbing components like methane, the adsorption isotherms are more linear, which results in a more linear dependence of the flux on feed (partial) pressure.

Table 2. Adsorption Parameters

	K_i 10^{-6} Pa^{-1}*		q_{sat} mmol·g^{-1}*
	Methane	Ethane	
273	7.0*	203*	1.92*
303	3.1	57	1.85
338	1.4	17	1.78
373	0.7	6.0	1.71
	Methane	Propane	
303	4.0	650	1.58

*Extrapolated from data at 303 K, 338 K, and 373 K.

Equation 6 is used to calculate the value of the diffusivity for each component from the single-component experiments. Table 1 lists the average value derived from experiments with different feed partial pressures at a given temperature. The lines in Figures 3a and 3b are calculated using this averaged diffusivity. The data in Table 1 are used to predict the permeation of binary mixtures through the membrane.

Binary mixture permeation

In Figures 4a and 4b the single-component ethane and methane fluxes (in the presence of helium) are compared to their flux in the presence of the other hydrocarbon. The flux of ethane is not altered by the presence of methane, but the methane flux is significantly reduced by ethane. This is typical for mixtures of fast, weakly adsorbing components (e.g., methane) and slow, strongly adsorbing components (e.g., ethane) that both easily fit into the zeolite channels (Bakker et al., 1996; Vroon, 1995; Van de Graaf et al., 1998a). For this kind of mixture separation is dominated by differences in adsorption. This feature can be attributed to micropore diffusion, where molecules are significantly hindered by the presence of the other components in the mixture. In the mixture the membrane is thus selective for ethane, which seems to have a blocking effect on methane. The extent of reduction of the methane flux by ethane is dependent on the ethane partial pressure, resulting in a composition-dependent selectivity. The higher the feed concentration of ethane, the more effective the reduction of the methane flux. Comparable features of mixture permeation through silicalite-1 membranes have been found for other systems such as propane/methane (this work), propene/ethene (Van de Graaf et al., 1998a), and *n*-butane/methane (Vroon, 1995).

Table 3. Membrane Parameters

Surface area membrane	2.0×10^{-4} m^2
Effective thickness of the zeolite layer	10×10^{-6} m
Density of the zeolite layer	1.8×10^{6} g·m^{-3}
Thickness of the support	3.0×10^{-3} m
Porosity of the support	0.2

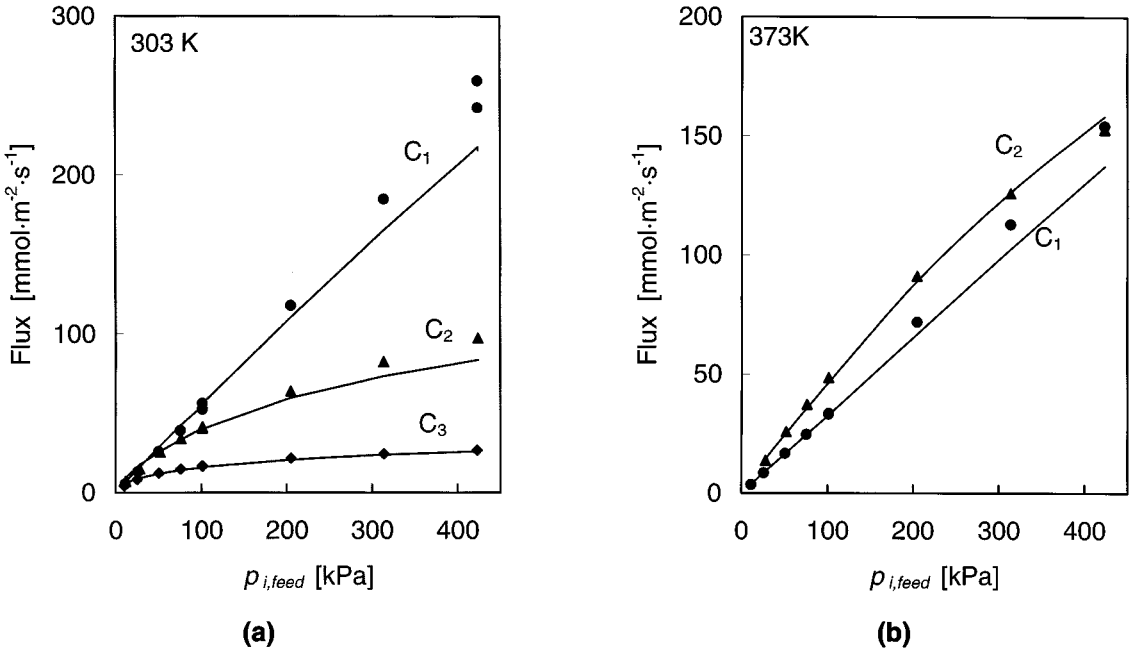

Figure 3. Permeation fluxes of methane (●), ethane (▲), and propane (♦) at 303 K (a) and 373 K (b) as a function of their feed partial pressure.

The lines are calculated using Eq. 6, using the values of $Đ_i^s$ listed in Table 1. Symbols represent experimental data.

The permeation of binary mixtures of ethane and methane was measured as a function of *composition, total hydrocarbon pressure,* and *temperature*. The results of these experiments are given in Figures 5–7, together with the predicted fluxes and selectivities using the GMS($Đ_{ij}^s = \infty$) model and the GMS model. The maximum in the flux of ethane (Figure 7) is the result of two opposite effects. The flux increases with temperature due to the activated nature of the diffusion process,

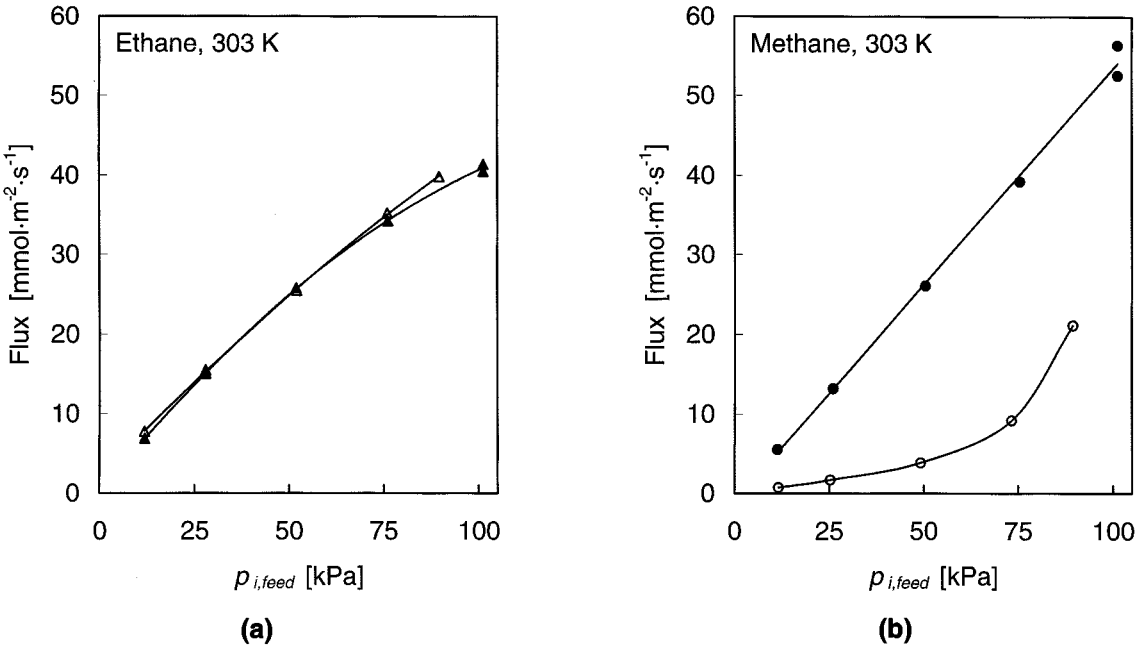

Figure 4. Permeation fluxes of ethane (a) and methane (b) at 303 K as a function of their feed partial pressure.

Closed symbols are single-component permeation experiments (balance helium); open symbols represent mixture permeation experiments (balance other hydrocarbon).

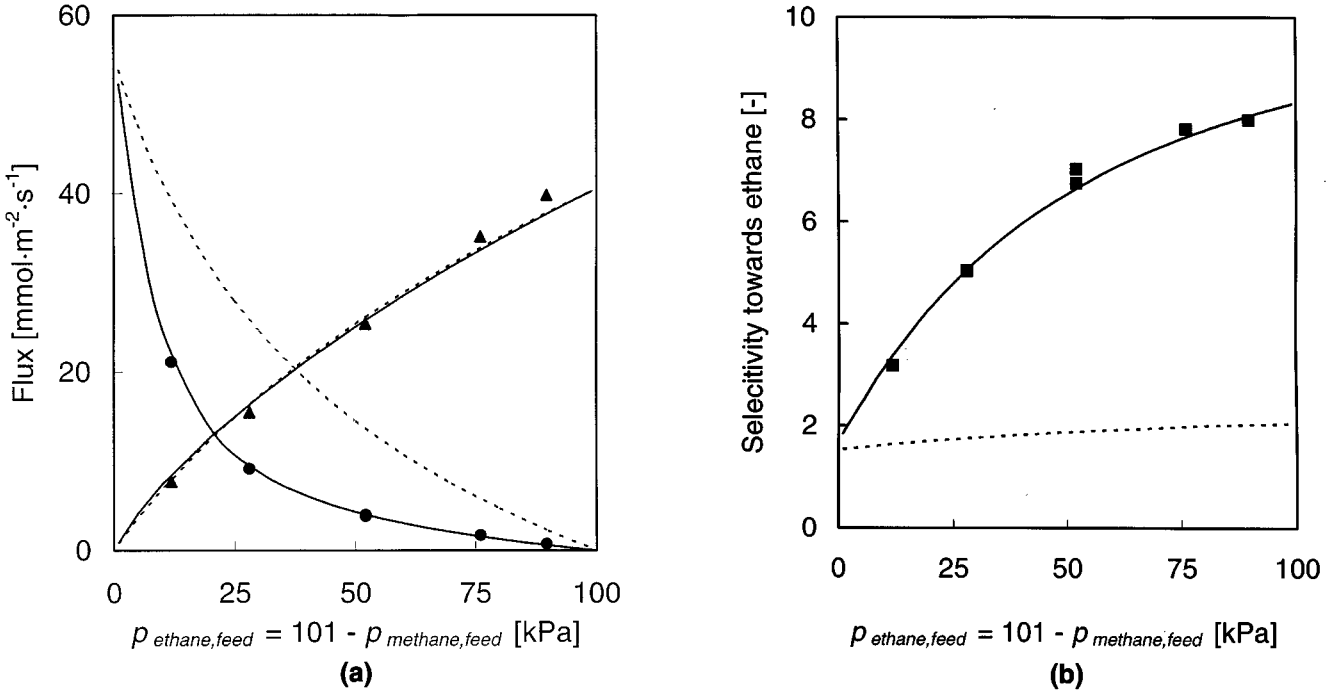

Figure 5. Ethane/methane mixture permeation fluxes (a) and selectivity toward ethane (b) as a function of the ethane feed partial pressure at 303 K.

The *composition* of the mixture changes from pure methane to pure ethane. Symbols: experimental data (ethane ▲, methane ●, selectivity ■); lines: model prediction (solid lines: GMS, dashed lines: GMS($Đ_{ij}^{s}=\infty$)).

but at a certain temperature the decrease in the adsorbed phase concentration becomes the limiting factor and the flux starts to decrease with temperature. The separation performance of the membrane is highly dependent on the operating conditions. High-feed partial pressures of ethane enhance the selectivity of the membrane (Figures 5 and 6). As the temper-

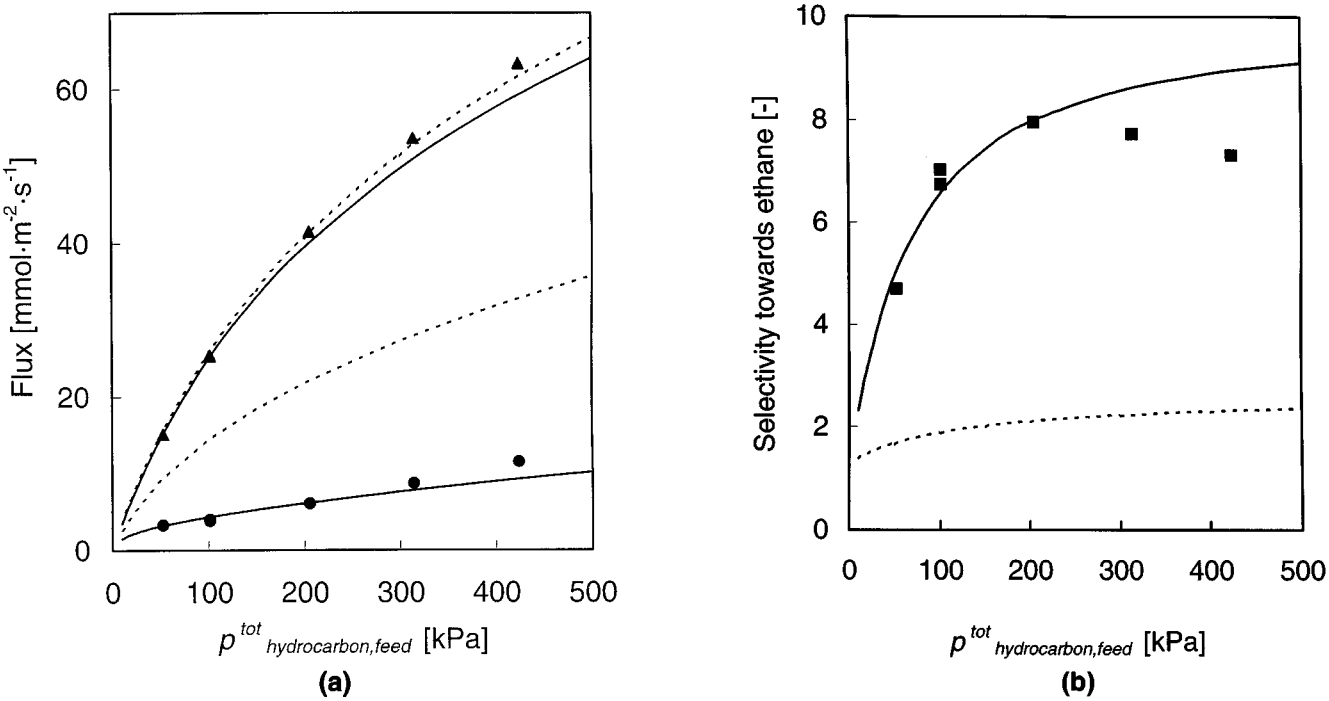

Figure 6. Ethane/methane mixture permeation fluxes (a) and selectivity toward ethane (b) as a function of the *total hydrocarbon feed pressure* (1:1 mixture) at 303 K.

Symbols: experimental data (ethane ▲, methane ●, selectivity ■); lines: model prediction (solid lines: GMS, dashed lines: GMS($Đ_{ij}^{s}=\infty$)).

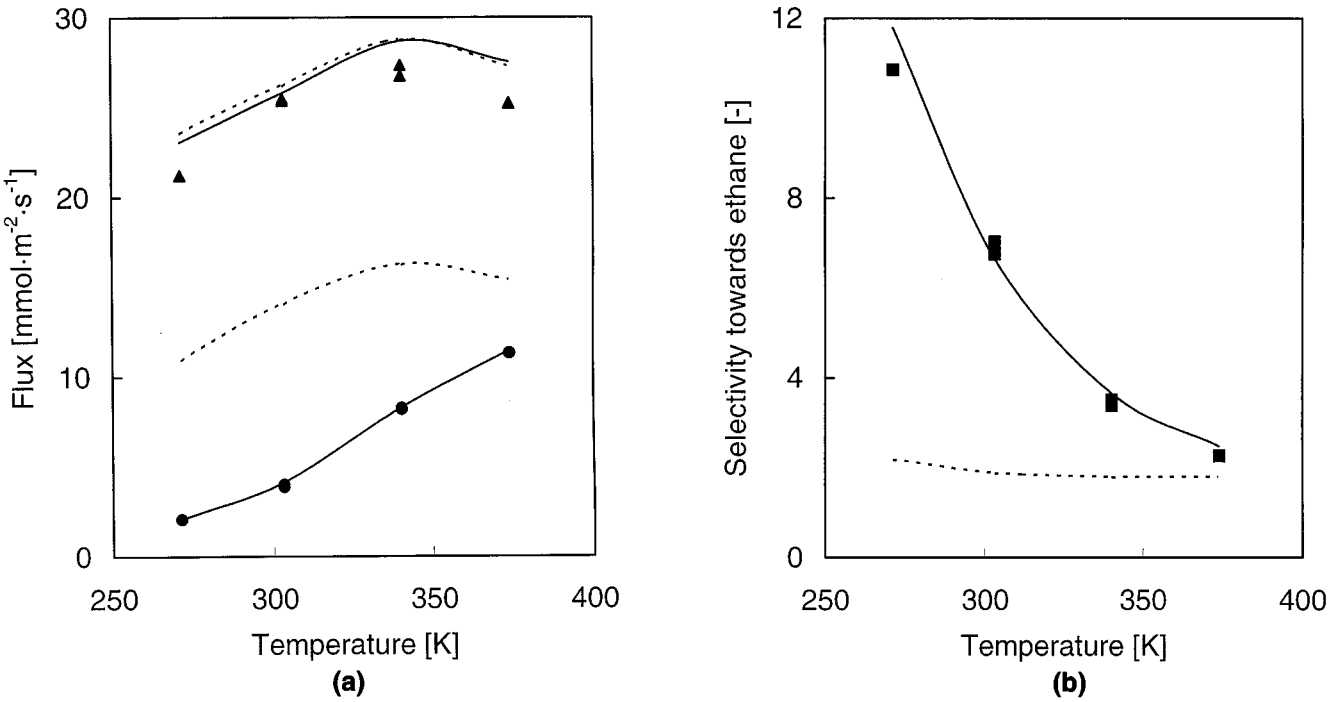

Figure 7. Ethane/methane mixture permeation fluxes (a) and selectivity toward ethane (b) as a function of *temperature* (1:1 mixture, p^{tot} = 101 kPa).

Symbols: experimental data (ethane ▲, methane ●, selectivity ■); lines: model prediction (solid lines: GMS, dashed lines: GMS($Đ_{ij}^s = \infty$)).

ature increases, the extent of reduction of the methane flux by ethane diminishes, since adsorption of ethane becomes weaker. As a result the selectivity toward ethane decreases with temperature from 10.9 at 273 K to 2.3 at 373 K (Figure 7).

The GMS model predicts the mixture permeation fluxes and selectivities very well. The GMS($Đ_{ij}^s = \infty$) model, assuming the absence of interaction between molecules, accurately predicts the ethane flux, but systematically overestimates the flux of methane. Consequently the GMS($Đ_{ij}^s = \infty$) model underestimates the membrane selectivity.

The permeation of mixtures of propane and methane with varying composition was also measured and predicted with the two Maxwell–Stefan models. The results are presented in Figure 8. Qualitatively, ethane/methane mixtures and propane/methane mixtures behave the same. The flux of the weakest adsorbing component (methane) is reduced by the presence of the strongest adsorbing component (propane), while the flux of the strongest component is unaltered in the mixture. The reduction of the methane flux by propane is more pronounced than by ethane, leading to selectivities of over 40. Again the selectivity found is dependent on the composition of the mixture, increasing with increasing propane content. The difference between the two model predictions is most pronounced for the methane flux, which is much lower when interaction between molecules is included. The GMS model predicts a selectivity toward propane of about 76 for a 1:1 mixture, whereas the GMS($Đ_{ij}^s = \infty$) model predicts a selectivity of only 5. Upon comparison with the experimental results, the GMS model is again superior to the GMS($Đ_{ij}^s = \infty$) model.

Simulation of transient permeation

The transient permeation of a mixture of propane (5 kPa) and methane (95 kPa) through the composite membrane was simulated using the GMS model and the GMS($Đ_{ij}^s = \infty$) model. The results of these simulations are given in Figure 9. In both models the flux of methane passes through a maximum as a function of time, but this maximum is more pronounced for the GMS model. The transient profile of propane is similar for both models. Under steady-state conditions the absolute value of the flux of methane is more than ten times higher for the GMS($Đ_{ij}^s = \infty$) model for the GMS model. In the latter case the methane flux is even lower than that of propane, in spite of the large methane excess in the gas phase.

Discussion

In this study the generalized Maxwell–Stefan equations are used to predict mixture permeation based on single-component adsorption and diffusion data, taking into account the proper local concentrations at the boundaries of the zeolite layer. This requires knowledge of (1) the concentration dependence of the single-component Maxwell–Stefan surface diffusivity; (2) the importance of adsorbate–adsorbate interactions; and (3) the prediction of the binary Maxwell–Stefan surface diffusivity, $Đ_{ij}^s$. These three issues are discussed in the following paragraphs.

Single-component diffusivities

If the single-component Maxwell–Stefan surface diffusivity, $Đ_i^s$, is independent of concentration, the single-component flux as a function of feed partial pressure can be de-

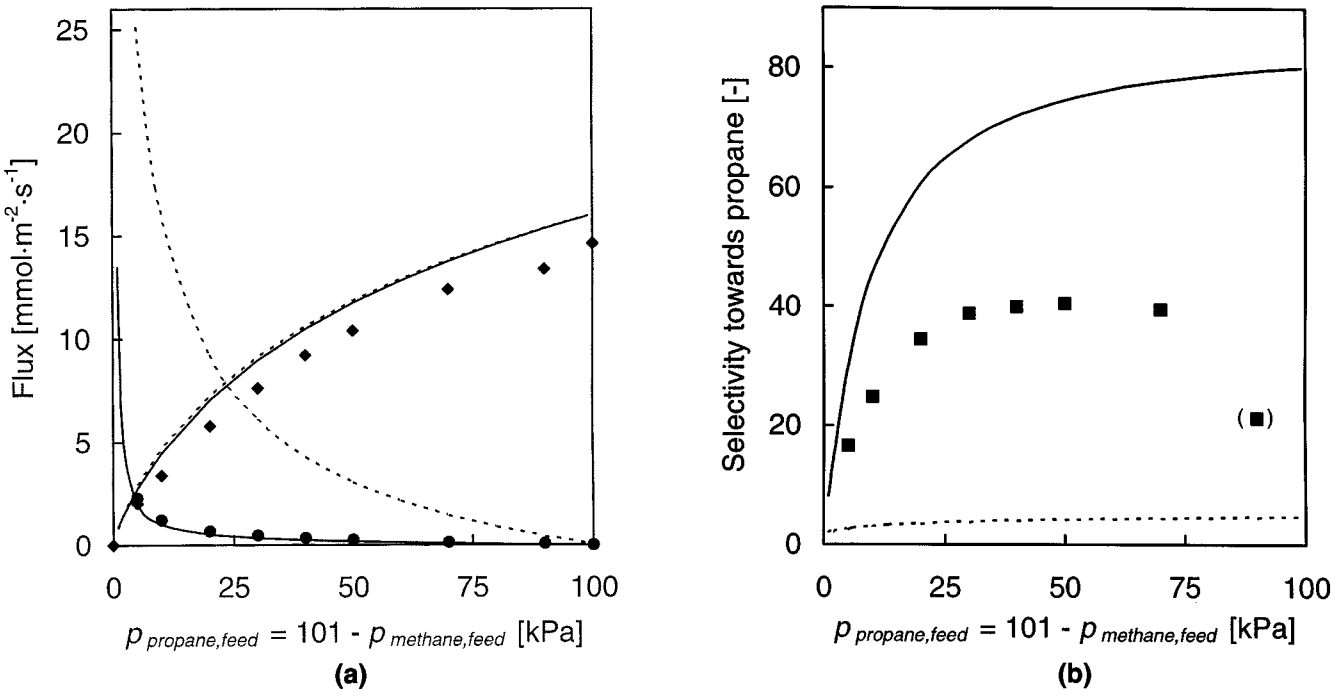

Figure 8. Propane/methane mixture permeation fluxes (a) and selectivity toward propane (b) as a function of the propane feed partial pressure.

The *composition* of the mixture changes from pure methane to pure propane. Symbols: experimental data (propane ♦, methane ●, selectivity ■); lines: model prediction (solid lines: GMS, dashed lines: GMS($Đ_{ij}^{s}=\infty$)).

scribed with a constant diffusivity using Eq. 6. As can be seen in Figures 3a and 3b, the assumption of a concentration-independent Maxwell–Stefan surface diffusivity is reasonable. Using a constant diffusivity, the single-component permeation fluxes can be described as having a maximum deviation of 25%.

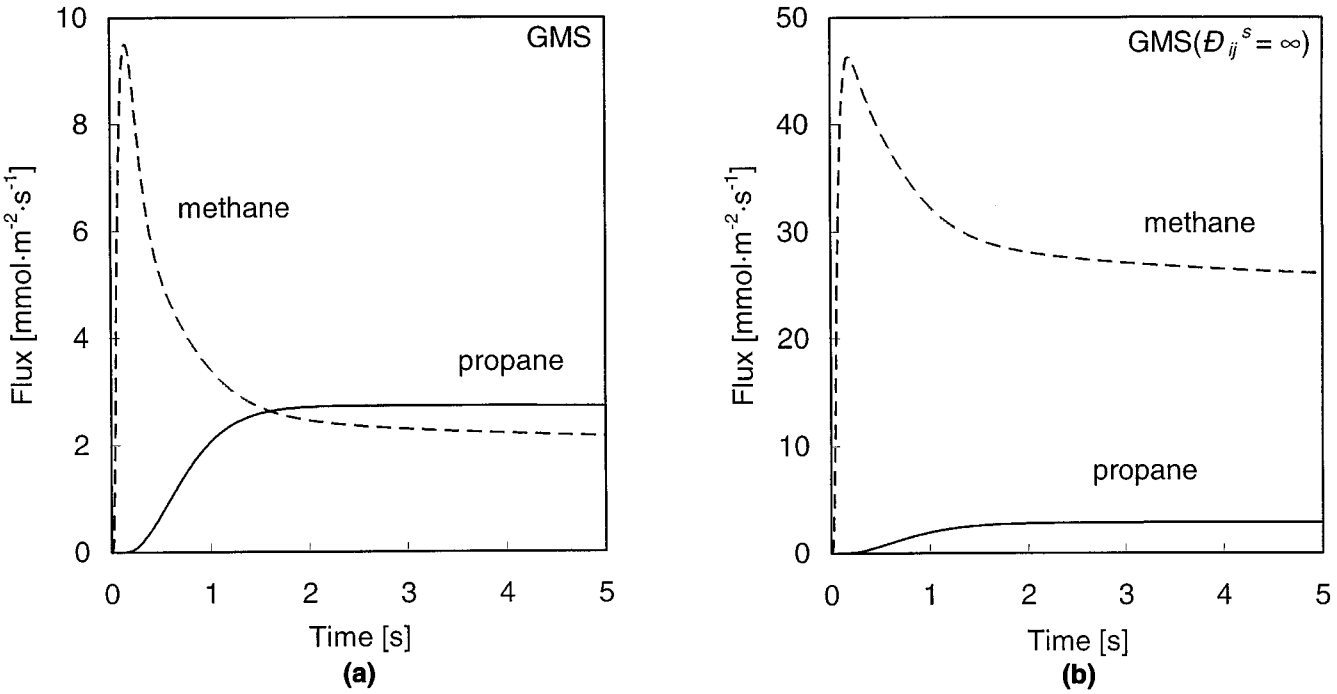

Figure 9. Simulation of the transient permeation, a mixture of methane (95 kPa, dashed line) and propane (5 kPa, solid line) through a silicalite-1 membrane at 303 K for the GMS model (a) and the GMS($Đ_{ij}^{s}=\infty$) model (b); parameters used are listed in Tables 1–3.

Prediction of mixture permeation

From the comparison of the experimental results and the predictions from both models, it is clear that the GMS model performs much better than the GMS($Đ_{ij}^s = \infty$) model, and that adsorbate–adsorbate interactions have to be included. The difference between the models is most significant when comparing the prediction of the methane flux with the different models. This flux is consistently overestimated in the GMS($Đ_{ij}^s = \infty$) model. Moreover, the GMS($Đ_{ij}^s = \infty$) model fails to describe the temperature dependence of the methane flux in the presence of ethane (Figure 7), even at a qualitative level. There is a good agreement between the fluxes and selectivities predicted with the GMS model and the experimental data. The predictions are based on single-component adsorption and diffusion data that were determined from separate adsorption and permeation experiments. No extra fitting parameters were involved in the model prediction.

The permeation flux of methane in the presence of propane is very small, especially at high propane partial pressures. It is therefore difficult to measure the methane flux under these experimental conditions, where its mass spectrometer signal barely exceeds the background value. The factor of 2 between the measured propane/methane selectivity and the predicted selectivity by the GMS model is attributed to the experimental error in the methane flux. This experimental error is also reflected in the data point at 90% propane in the feed, where the experimentally determined selectivity suddenly dropped considerably.

In view of the results, it can be concluded that the empirical Vignes relation provides a good approximation for the binary Maxwell–Stefan surface diffusivity, $Đ_{ij}^s$. According to Eq. 9, the value of $-D_{12}^s$ is always in between the value of $Đ_1^s$ and $Đ_2^s$, and it varies with the concentration of both components. At the retentate side of the membrane the relative concentration of the weakly adsorbing component is higher than at the permeate side of the membrane where this component is hardly present. This means that the value of $Đ_{12}^s$ has the highest value at the feed side. In Figures 10a and 10b the value of $Đ_{12}^s$, averaged over the membrane, for ethane/methane and propane/methane mixtures as a function of the composition of the feed mixture is shown, as are the single-component diffusivities. The value of $Đ_{12}^s$ is highly dependent on the composition of the mixture. The value of $Đ_{12}^s$ is closest to that of the strongest adsorbing component, except at very low (< 10 kPa) partial pressures of this component. The selectivity toward methane, which is the inverse of the selectivity toward ethane or propane, is also given in the same figure. The composition dependence of the selectivity follows a similar trend as the composition dependence of $Đ_{12}^s$. The interpretation of this is discussed later.

Transient permeation of *n*-butane/methane mixtures and *n*-butane/hydrogen mixtures shows a maximum in the flux of the fast, weakly adsorbing component (methane and hydrogen, respectively) before steady state is reached (Bakker et al., 1993, 1996). This maximum is explained as follows. Initially, the zeolite membrane is empty and the fluxes are proportional to the independent mobilities of the components in the zeolite lattice. As time proceeds, the fast, weakly adsorbing component is replaced by the slow, strongly adsorbing

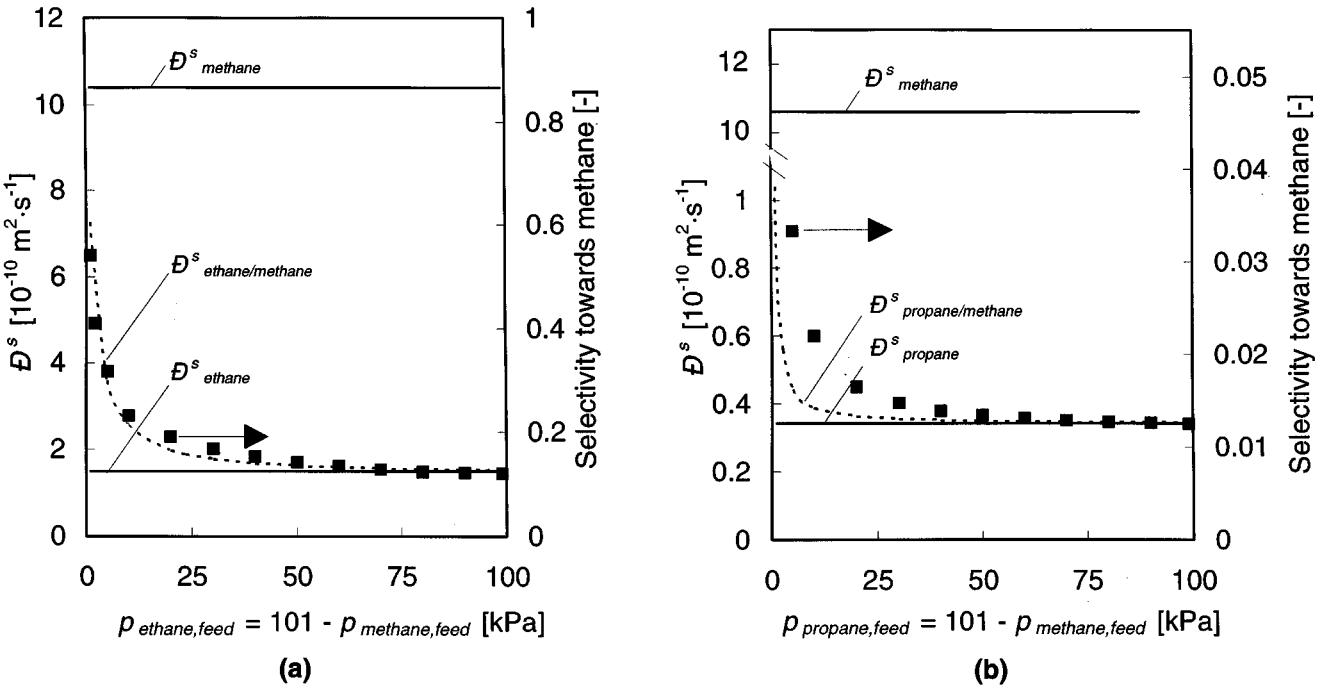

Figure 10. The average Maxwell–Stefan binary surface diffusivity, $Đ_{ij}^s$, and the selectivity (■) toward methane, as a function of the composition of (a) ethane/methane mixtures and (b) propane/methane mixtures at 303 K ($p^{tot} = 101$ kPa).

The *composition* of the mixture changes from pure methane to pure ethane or propane. The single-component Maxwell–Stefan diffusivities ($Đ_i^s$) are also shown.

component that will have a blocking effect on the permeation of the weakly adsorbing component. This results in a decline in the permeation flux of the fast, weakly adsorbing component. This is analogous to what is observed for transient uptake experiments in zeolite crystals, where the uptake of the fast, weakly adsorbing components often goes through a maximum as a function of time (Habgood, 1958; Kärger and Bülow, 1975; Niessen and Karge, 1993).

Krishna and Van den Broeke (1995) already showed that for the simulation of the transient permeation of mixtures through zeolite membranes, the mathematical description of the fluxes should be based on the chemical potential gradient as the driving force for diffusion. The qualitative trends as described earlier could not be simulated using the simple Fickian model, based on the concentration gradient as the driving force for diffusion. Krishna and Van den Broeke used the GMS($Đ_{ij}^s = \infty$) model to describe the results of Bakker et al. (1993, 1996). Although the maximum in the flux was qualitatively predicted, the ratio between the maximum in the flux and the steady-state value of the flux was always too low. In Figure 9 the simulation results of the transient permeation of a propane/methane mixture obtained with the GMS model and the GMS($Đ_{ij}^s = \infty$) model are compared. The transient profiles of the weakly adsorbing component are distinctly different. The ratio between the maximum in the flux of methane and its steady-state value is much higher for the GMS model, which is more in agreement with the experimental results. This gives good perspectives for the quantitative modeling of transient permeation fluxes through zeolite membranes. At present the calculated transient permeation profiles cannot be correlated to experimental results, since this requires detailed knowledge of the response time of the permeation equipment and the permeate and retentate volumes, which is not available at the moment.

Comparison between the GMS and GMS($Đ_{ij}^s = \infty$) models

The difference between the GMS model and the GMS($Đ_{ij}^s = \infty$) models becomes very clear if the limits of the models are compared. Consider a mixture of a fast, weakly adsorbing component (1) and a slow, strongly adsorbing component (2), then

$$Đ_1^s > Đ_2^s \qquad \text{and} \qquad \theta_1 < \theta_2, \tag{12}$$

and, from Eq. 9

$$\frac{Đ_{12}^2}{Đ_2^s} \sim 1. \tag{13}$$

Using Eq. 13, Eq. 7 can be rewritten to Eq. 14 for the fast component

$$N_1^s = -q_{sat}\rho \frac{Đ_{12}^s}{(1-\theta_1-\theta_2)} \frac{\left[(1-\theta_2)+\theta_1\right]\nabla\theta_1 + \left[2\theta_1\right]\nabla\theta_2}{\theta_2}. \tag{14}$$

This explains the observation that the composition dependence of the selectivity follows a similar trend as the composition dependence of $Đ_{12}^s$ (Figure 10). With increasing concentration of the strongest adsorbing component 2, $Đ_{12}^s$ decreases, and consequently the flux of component 1 diminishes and the selectivity toward component 2 increases.

In the limit $Đ_{12}^s$ equals $Đ_2^s$ (Figure 10), and the flux of the fast, weakly adsorbing component is determined by its own concentration (gradient), the concentration (gradient) of the other component, and the diffusivity of the slow, strongly adsorbing component. So, the maximum flux of component 1 can never exceed a certain value, even if its own diffusivity is infinitely high. In the GMS($Đ_{ij}^s = \infty$) model (Eq. 8) the flux of the fastest component increases linearly and unlimited with its diffusivity. The restriction of the flux of component 1 by component 2 in this model is exclusively controlled by the coadsorption of component 2 in the zeolite and not by changes in the mobility of component 1.

For the slow component 2 it can be assumed that $\theta_2 Đ_1^s/Đ_{12}^s$ is the most significant term in the denominator of Eq. 7. For this component the flux can be approximated by

$$N_2^s = -q_{sat}\rho \frac{Đ_2^s}{(1-\theta_1-\theta_2)}\left[\nabla\theta_1 + \nabla\theta_2\right]. \tag{15}$$

For the model system chosen here, θ_1 is small and θ_2 is close to unity. This means that Eq. 15 is almost identical to the GMS($Đ_{ij}^s = \infty$) model (Eq. 8). This shows why there is little difference between the fluxes of the slow, strongly adsorbing component predicted by the two models.

In the narrow channels of the zeolite the molecules are unable to pass each other. If the zeolite framework is highly occupied with the slow component 1, it is expected that component 2 is slowed down considerably, even if its own mobility is high. This physical picture is only reflected in the complete GMS model.

Several PFG-NMR studies on the diffusion of mixtures of hydrocarbons in zeolites have been conducted to assess the mobility of one component in the presence of another. Using this technique, the self-diffusivity (diffusivity in the absence of an applied concentration gradient) of each component is measured, keeping the concentration of the component under study the same. Examples are the diffusion of ethane/ethene mixtures in zeolite NaX (Hong et al., 1991), methane/ethene in NaY (Nivarthi and McCormick, 1995; Nivarthi et al., 1995), ethane/ethene in silicalite (Nivarthi and McCormick, 1995), methane/benzene in NaY (Nivarthi et al., 1995), and methane/tetrafluoromethane in silicalite (Snurr and Kärger, 1997). In all studies, except the latter, it was found that the self-diffusivity of the fastest component decreased in the presence of a slow component reaching a value close to that of the slow component. The self-diffusivity of the slow component was not altered by the presence of the fast component. In the study of Snurr and Kärger (1997) it was found that the mobility of both components decreased in the mixture. In all PFG-NMR studies the self-diffusivities of the components were closer to each other in the mixture than in the single-component measurements. The PFG-NMR results are in agreement with the physical picture presented in the previous paragraph and the complete GMS model. The experimental fluxes through the silicalite-1 membrane are also in agreement with this representation. In the mixture, the flux

of the fastest component decreased, whereas the flux of the slow component remained constant.

Based on the preceding it has to be concluded that the GMS($Đ_{ij}^s = \infty$) model is not only unable to predict the experimentally observed mixture permeation fluxes quantitatively, it is also physically unrealistic.

Selectivity in membrane-based separations

According to the experimental results and the model calculations, a maximum selectivity is thus obtained at the high occupancy. Based on the complete GMS model, the highest achievable selectivity with the membrane can be predicted. For high total pressures the total occupancy approaches unity

$$\theta_1 + \theta_2 \to 1 \;\Rightarrow\; 1 - \theta_1 \to \theta_2,\; 1 - \theta_2 \to \theta_1. \tag{16}$$

For an equimolar mixture the selectivity can be approximated by the ratio between the fluxes. Upon combining Eqs. 7, 13, and 16, the selectivity obtained for an equimolar mixture of component 1 (fast, weakly adsorbing) and component 2 (slow, strongly adsorbing) can be expressed as Eq. 17

$$\lim_{\theta_1 + \theta_2 \to 1} \alpha_{21} = \frac{\theta_2}{\theta_1} \frac{1 + \dfrac{Đ_{12}^s}{Đ_1^s}}{2}. \tag{17}$$

For the fictive mixture under consideration $Đ_{12}^s$ is much smaller than $Đ_1^s$, so the maximum achievable selectivity is close to $\theta_1/(2 \cdot \theta_2)$ (Eq. 18)

$$\underbrace{\alpha_{21}^{max} = \frac{\theta_2}{\theta_1}\frac{1}{2}}_{\text{Membrane-based separation}} \qquad \underbrace{\alpha_{21}^{max} = \frac{\theta_2}{\theta_1}.}_{\text{Equilibrium adsorption-based separation}} \tag{18}$$

For ethane/methane and propane/methane mixtures the maximum selectivity, calculated with Eq. 19, corresponds to 9.2 and 81 at 303 K, respectively. This is indeed close to the selectivity simulated with the GMS model near saturation of the zeolite (Figures 6b and 7b). For separation processes, based on equilibrium adsorption the selectivity is equal to θ_1/θ_2, a factor of 2 higher than in the membrane separation process. This is caused by the fact that, for the mixtures under consideration, adsorption and diffusion counteract each other. From a selectivity point of view, adsorption-based separation processes are thus more favorable for this kind of mixtures. The separation selectivity is, however, only one aspect of a separation process; other factors, like the ease and mode of operation of the process, will also determine which separation process is most suitable for a specific application.

For very low occupancies it can be shown that the selectivity is equal to the product of diffusion and adsorption selectivity (Eq. 19)

$$\theta_1, \theta_2 \to 0 \qquad \frac{N_2}{N_1} = \frac{Đ_2^s}{Đ_1^s} \cdot \frac{\nabla\theta_2}{\nabla\theta_1} \;\Rightarrow\; \alpha_{21} = \frac{Đ_2^s}{Đ_1^s} \cdot \frac{K_2}{K_1}. \tag{19}$$

Final remarks

The term single-file diffusion refers to the situation where molecules are not able to pass each other in the pore, and molecules can only move if the next adsorption site is vacant (Sholl and Fichthorn, 1997; Riekert, 1971). In the work of Krishna (1993) the binary Maxwell–Stefan surface diffusivity $Đ_{ij}^s$ is interpreted as a counterexchange diffusion coefficient, which represents the possibility of molecules exchanging place on the surface. Since this is not likely in the narrow zeolite pores, $Đ_{ij}^s$ was assumed to be infinite and friction between molecules is neglected (Krishna and Van den Broeke, 1995). The interpretation of $Đ_{ij}^s$ as a "counterexchange" coefficient is confusing, since the fact that molecules cannot exchange places in the pore, does not mean that they do not experience each others presence. A slow molecule will slow down a faster molecule and vice versa. The results presented here show that because the molecules cannot pass each other, they have to move in a single file and their mobility becomes identical. This is reflected in the binary surface diffusivity $Đ_{ij}^s$. The interpretation of the Maxwell–Stefan diffusivities as inverse drag coefficients, as proposed by Krishna (1993), is much more amenable for this physical interpretation.

This study presents a good model description of mixture permeation through zeolite membranes and provides experimental evidence in favor of the complete GMS model to describe mixture permeation. It is, however, noted that the systems studied here are relatively simple in the sense that adsorption of methane, ethane, and propane follows the Langmuir isotherm, and their single-component diffusivities were almost independent of concentration. The adsorption characteristics of molecules like *i*-butane and larger hydrocarbons are much more complex (Zhu et al., 1998; Smit and Maessen, 1995; Vlugt et al., 1998), due to the preferential packing of these molecules in the zeolite framework. This preferential packing is reflected in a step or kink in the adsorption isotherm. More complex adsorption isotherms, like the dual-site Langmuir model, are then required to relate pressures to adsorbed phase concentration. This results in a more complex form of the thermodynamic factor (Krishna et al., 1998). Moreover, knowledge about adsorption of mixtures of these components is still lacking while information about the concentration of components in the zeolite is essential for the description of diffusion in zeolite membranes. This makes it difficult at present to model permeation of the mixture of components that exhibit peculiar adsorption behavior.

Conclusions

Separation of the mixtures of hydrocarbons by the silicalite-1 membrane used in this study is dependent on composition, total pressure, and temperature. Depending on the operating conditions, the silicalite-1 membrane exhibited a selectivity for ethane/methane mixtures between 10.9 and 2.2 in favor of ethane. The selectivity toward propane in propane/methane mixtures varies between 16.6 and 40.5, under the experimental conditions in this study.

Permeation of ethane/methane and propane/methane mixtures as a function of composition, total hydrocarbon pressure, and temperature was predicted using the generalized Maxwell–Stefan equations applied to surface diffusion. The model predictions, based on separately determined sin-

gle-component adsorption and diffusion parameters, were in excellent agreement with the experimental data. Using the empirical Vignes relation for the prediction of the binary Maxwell–Stefan surface diffusivity, there were no fitting parameters involved in the model prediction.

For a mixture of a fast, weakly adsorbing component and a slow, strongly adsorbing component it was found that flux of the weakly adsorbing component is reduced significantly compared to its single-component flux. The flux of the strongest adsorbing component hardly changes due to the presence of the weakly adsorbing component. The complete Maxwell–Stefan model, including adsorbate–adsorbate interaction, describes the flux reduction of the weakly adsorbing component quantitatively much better than the model in which these interactions are neglected. The latter model systematically overestimates the flux of the weakly adsorbing component, thus predicting a too low selectivity. Also transient binary permeation phenomena are much better described by the complete Maxwell–Stefan model. The present data show unequivocally that adsorbate–adsorbate interactions have to be included in the description of mixture permeation through zeolite membranes.

Theoretical analysis showed that for systems of fast, weakly adsorbing components and slow, strongly adsorbed component the maximum selectivity obtained with microporous membrane separation is always a factor of 2 lower than the one obtained under equilibrium adsorption conditions.

Notation

A = membrane surface area, m^2
K = adsorption constant, Pa^{-1}
N = flux in the support layer, $mol \cdot m^2 \cdot s^{-1}$
N^s = surface flux in the zeolite layer, $mol \cdot m^2 \cdot s^{-1}$
m = molar mass, $g \cdot mol^{-1}$
p = pressure, Pa
q = adsorbed phase concentration in the zeolite, $mol \cdot g^{-1}$
R = gas constant, $J \cdot mol^{-1} \cdot K^{-1}$
T = temperature, K

Greek letters

ϵ = porosity of the support
Γ = thermodynamic factor
ϕ = flow rate, $mol \cdot s^{-1}$
ρ = density, $g \cdot m^{-3}$

Subscripts/superscripts

he = helium
i, j, 1, 2 = component *i, j,* 1, 2
feed = feed
tot = total

Literature Cited

Abdule-Rehman, H. B., M. A. Hasanain, and K. F. Loughlin, "Quaternary, Ternary, Binary and Pure Component Sorption on Zeolites. 1. Light Alkanes on Linde S-115 Silicalite at Moderate to High Pressures," *Ind. Eng. Chem. Res.*, **29**, 1525 (1990).

Bakker, W. J. W., G. Zheng, F. Kapteijn, M. Makkee, J. A. Moulijn, E. R. Geus, and H. van Bekkum, "Single and Multi-Component Transport Through Metal-Supported MFI Zeolite Membranes," *Precision Process Technology*, M. P. C. Weijnen and A. A. H. Drinkenburg, eds., Kluwer, Dordrecht, The Netherlands, p. 425 (1993).

Bakker, W. J. W., F. Kapteijn, J. Poppe, and J. A. Moulijn, "Permeation Characteristics of a Metal Supported Silicalite-1 Zeolite Membrane," *J. Membr. Sci.*, **117**, 57 (1996).

Bakker, W. J. W., L. P. J. van den Broeke, F. Kapteijn, and J. A. Moulijn, "Temperature Dependence of One-Component Permeation Through a Silicalite-1 Membrane," *AIChE J.*, **43**(9), 2203 (1997).

Broughton, B. R., "Adsorption Isotherms for Binary Gas Mixtures," *Ind. Eng. Chem.*, **40**(8), 1506 (1948).

Chem. Eng. J., **57** (1995) (Special Issue).

Chen, Y. D., and R. T. Yang, "Predicting Binary Fickian Diffusivities from Pure-Component Fickian Diffusivities for Surface Diffusion," *Chem. Eng. Sci.*, **47**, 3895 (1992).

Chen, Y. D., and R. T. Yang, "Preparation of Carbon Molecular Sieve Membrane and Diffusion of Binary Mixtures in the Membrane," *Ind. Eng. Chem. Res.*, **33**, 3146 (1994).

Füller, E. N., P. D. Schettler, and J. C. Giddings, "A New Method for the Prediction of Gas Phase Diffusion Coefficients," *Ind. Chem. Eng.*, **58**, 19 (1996).

Funke, H. H., M. G. Kovalchick, J. L. Falconer, and R. D. Noble, "Separation of Hydrocarbon Isomer Vapors with Silicalite Zeolite Membranes," *Ind. Eng. Chem. Res.*, **35**, 1575 (1996).

Geus, E. R., H. van Bekkum, W. J. W. Bakker, and J. A. Moulijn, "High-Temperature Stainless-Steel Supported Zeolite (MFI) Membranes: Preparation, Module Construction, and Permeation Experiments," *Microporous Mater.*, **1**, 131 (1993).

Habgood, H. W., "The Kinetics of Molecular Sieve Action: Sorption of Nitrogen Methane Mixtures by Linde Molecular Sieve 4A," *Can. J. Chem.*, **36**, 1384 (1958).

Hong, U. W., J. Kärger, and H. Pfeifer, "Selective Two-Component Self Diffusion Measurement of Adsorbed Molecules by Pulsed Field Gradient Fourier Transform NMR," *J. Amer. Chem. Soc.*, **113**, 4812 (1991).

Jia, M.-D., B. Chen, R. D. Noble, and J. L. Falconer, "Ceramic-Zeolite Composite Membranes and their Application for Separation of Vapor/Gas Mixtures," *J. Membr. Sci.*, **90**, 1 (1994).

Kapteijn, F., W. J. W. Bakker, G. Zheng, J. Poppe, and J. A. Moulijn, "Permeation and Separation of Light Hydrocarbons through a Silicalite-1 Membrane. Application of the Generalized Maxwell–Stefan Equations," *Chem. Eng. J.*, **57**, 145 (1995).

Käger, J., and M. Bülow, "Theoretical Prediction of Uptake Behavior in Adsorption Kinetics of Binary Gas Mixtures Using Irreversible Thermodynamics," *Chem. Eng. Sci.*, **30**, 893 (1975).

Käger, J., and D. M. Ruthven, *Diffusion in Zeolites and Other Microporous Solids*, Wiley, New York (1992).

Karpoor, A., and R. T. Yang, "Kinetic Separation of Methane-Carbon Dioxide Mixture by Adsorption on Molecular Sieve Carbon," *Chem. Eng. Sci.*, **44**(8), 1723 (1989).

Knoblauch, K., "Pressure-Swing Adsorption: Geared for Small-Volume Users," *Chem. Eng.*, 87 (Nov. 6, 1978).

Knoblauch, K., H. Heimbach, and B. Harder, "Process for Recovering Nitrogen from Oxygen-Containing Gas Mixtures," U.S. Patent No. 4,548,799 (1985).

Krishna, R., "Multicomponent Surface Diffusion of Adsorbed Species: A Description Based on the Generalized Maxwell-Stefan Equations," *Chem. Eng. Sci.*, **45**(7), 1779 (1990).

Krishna, R., "A Unified Approach to the Modeling of Intraparticle Diffusion in Adsorption Processes," *Gas Sep. Purif.*, **7**(2), 91 (1993).

Krishna, R., and L. J. P. van den Broeke, "The Maxwell-Stefan Description of Mass Transport Across Zeolite Membranes," *Chem. Eng. J.*, **57**, 155 (1995).

Krishna, R., T. J. H. Vlugt, and B. Smit, "Sorption-Induced Diffusion-Selective Separation of Hydrocarbon Isomers Using Silicalite," *J. Phys. Chem. A*, **102**(40), 7727 (1998).

Krylov, S. Y., A. V. Prosyanov, and J. J. M. Beenakker, "One Dimensional Surface Diffusion. II. Density Dependence in a Corrugated Potential," *J. Chem. Phys.*, **170**, 6970 (1997).

Kusakabe, K., S. Yoneshige, A. Murata, and S. Morooka, "Morphology and Gas Permeance of ZSM-5 Type Zeolite Membrane Formed on a Porous α-Alumina Support Tube," *J. Memb. Sci.*, **116**, 39 (1996).

Kusakabe, K., T. Kuroda, A. Murata, and S. Morooka, "Formation of a Y-Type Zeolite Membrane on a Porous α-Alumina Tube for Gas Separation," *Ind. Eng. Chem. Res.*, **36**, 649 (1997).

Kusakabe, K., T. Kuroda, and S. Morooka, "Separation of Carbon

Dioxide from Nitrogen Using Ion-Exchanged Faujasite-Type Zeolite Membranes Formed on Porous Support Tubes,'' *J. Membr. Sci*., **148**, 13 (1998).
Meyers, A. L., and J. M. Prausznitx, ''Thermodynamics of Mixed Gas Adsorption,'' *AIChE J*., **11**, 121 (1965).
Niessen, W., and H. G. Karge, ''Diffusion of *p*-Xylene in Single and Binary Systems in Zeolites Investigated by FTIR Spectroscopy,'' *Microporous Mater*., **1**, 1 (1993).
Nivarthi, S. S., and A. V. McCormick, ''Diffusion of Co-Adsorbed Molecules in Zeolites: A Pulsed Field Gradient NMR Study,'' *J. Phys. Chem*., **99**, 4661 (1995).
Nivarthi, S. S., H. T. Davis, and A. V. McCormick, ''Effectiveness of Window Blocking in Zeolite NaY by Strongly Coadsorbed Molecules,'' *Chem. Eng. Sci*., **50**, 3217 (1995).
Poshusta, J. C., V. A. Tuan, J. L. Falconer, and R. D. Noble, ''Synthesis and Permeation Properties of SAPO-34 Tubular Membranes,'' *Ind. Eng. Chem. Res*., **37**, 3924 (1998).
Rao, M. B., and S. Sircar, ''Nanoporous Carbon Membranes for Separation of Gas Mixtures by Selective Surface Flow,'' *J. Membr. Sci*., **85**, 253 (1993).
Riekert, L., ''Rates of Sorption and Diffusion of Hydrocarbons in Zeolites,'' *AIChE J*., **17**(2), 446 (1971).
Sholl, D. S., and K. A. Fichthorn, ''Normal, Single-File, and Dual Mode Diffusion of Binary Adsorbate Mixtures in $AlPO_4$-5,'' *J. Chem. Phys*., **170**(11), 4384 (1997).
Smit, B., and T. L. Maessen, ''Commensurate 'Freezing' of Alkanes in the Channels of a Zeolite,'' *Nature*, **374**, 42 (1995).
Snurr, R. Q., and K. Kärger, ''Molecular Simulations and NMR Measurements of Binary Diffusion in Zeolites,'' *J. Phys. Chem*., **101**, 6469 (1997).
Tuchlenski, A., P. Uchytil, and A. Seidel-Morgenstern, ''An Experimental Study of Combined Gas Phase and Surface Diffusion in Porous Glass,'' *J. Membr. Sci*., **140**, 165 (1998).
Van de Graaf, J. M., F. Kapteijn, and J. A. Moulijn, ''Effect of Operating Conditions and Membrane Quality on Separation Performance of Composite Silicalite-1 Membranes,'' *Ind. Eng. Chem. Res*., **10**, 4071 (1998a).
Van de Graaf, J. M., F. Kapteijn, and J. A. Moulijn, ''Methodological and Operational Aspects of Permeation Measurements on Silicalite-1 Membranes,'' *J. Membr. Sci*., **144**(1–2), 87 (1998b).
Van de Graaf, J. M., ''Transport and Separation Properties of Supported Silicalite Membranes. A Modeling Approach,'' PhD Thesis, Delft Univ. of Technology, Delft, The Netherlands (1998c).
Van den Broeke, L. J. P., ''Simulation of Diffusion in Zeolitic Structures,'' *AIChE J*., **41**, 2399 (1995).
Vignes, A., ''Diffusion in Binary Solutions,'' *Ind. Eng. Chem. Fundam*., **5**(2), 189 (1966).
Vlugt, T. J. H., W. Zhu, F. Kapteijn, J. A. Moulijn, B. Smit, and R. Krishna, ''Adsorption of Linear and Branched Alkanes in the Zeolite Silicalite-1,'' *J. Amer. Chem. Soc*., **120**, 5599 (1998).
Vroon, Z. A. E. P., ''Synthesis and Transport Studies of Thin Ceramic Supported Zeolite (MFI) Membranes,'' PhD Thesis, Twente Univ. of Technology, Enscheede, The Netherlands (1995).
Vroon, Z. A. E. P., K. Keizer, M. J. Gilde, H. Verweij, and A. J. Burggraaf, ''Transport Properties of Alkanes through Ceramic Thin Zeolite MFI Membranes,'' *J. Membr. Sci*., **113**, 293 (1996).
Vroon, Z. A. E. P., K. Keizer, A. J. Burggraaf, and H. Verweij, ''Preparation and Characterization of Thin Zeolite MFI Membranes,'' *J. Membr. Sci*., **144**, 77 (1998).
Wesseling, J. A., and R. Krishna, *Mass Transfer*, Ellis Horwood Series in Chemical Engineering, Ellis Horwood Ltd., Chichester (1990).
Yang, R. T., Y. D. Chen, and Y. T. Yeh, ''Prediction of Cross-Term Coefficients in Binary Diffusion: Diffusion in Zeolite,'' *Chem. Eng. Sci*., **46**, 3089 (1991).
Zhu, W., J. M. van de Graaf, L. P. J. Van den Broeke, F. Kapteijn, and J. A. Moulijn, ''TEOM: A Unique Technique for Measuring Adsorption Properties: Light Alkanes in Silicalite-1,'' *Ind. Eng. Chem. Res*., **37**, 1934 (1998).

Manuscript received Aug. 23, 1998, and revision received Nov. 23, 1998.